UNRAVELING DYNAMIC MECHANICAL DEFORMATION IN SEGMENTED POLYURETHANES: FROM HIGH STRAIN-RATE HARDENING TO COMPLETE FOLD RECOVERY

A. J. Hsieh*
U. S. Army Research Laboratory, AMSRD-ARL-WM-MD
Aberdeen Proving Ground, MD 21005-5069

J. Yi[1], B. D. Pate[2], M. C. Boyce[1,2]
[1]Department of Mechanical Engineering and [2]Institute for Soldier Nanotechnologies
Massachusetts Institute of Technology, Cambridge, MA 02139

ABSTRACT

In light of the increased threat from terrorist activities in recent years, there is a critical need for lightweight transparent ballistic shield materials that are mechanically robust and have multi-functional properties. Transparent segmented polyurethanes (PU) in particular have shown potential for use as rigid ballistic shields and as lens materials for flexible C/B protective face masks. The performance specifications required for each application are quite different, and the current state-of-the-art PU technology can not completely fulfill the full spectra of materials survivability including the simultaneous mechanical and chemical hardening against the emerging operational threats. ARL is currently engaged in collaboration with the Institute for Soldier Nanotechnologies (ISN) to investigate and exploit new molecular mechanisms for design of novel hierarchical hybrid structures to achieve the desired physical and mechanical properties. This paper presents the experimental findings from recent studies conducted at the ISN whereby the role of molecular structures on the dynamic mechanical deformation of a model set of segmented polyurethanes was determined. The microphase morphology, thermal transitions, molecular relaxation, and mechanical deformation were investigated. The nature of chain extender significantly affected the extent of phase mixing between the hard and soft segments: incorporation of 2,2-dimethyl-1,3-propanediol (DMPD) as the chain extender resulted in a 51°C increase in the soft segment T_g relative to the analogous 1,4-butanediol (BDO)-containing PU samples. Small-angle X-ray scattering data indicated that the structure difference between chain extenders was correlated with a substantial change in interdomain structure. The BDO-containing PU samples exhibited a single, broad scattering peak that is typical of phase-segregated segmented polyurethanes; in contrast, no characteristic interdomain spacing was observed in the highly phase-mixed, sterically encumbered DMPD-containing samples. Moreover, the extent of physical mixing drastically affected the mechanical deformation of these model segmented PU materials whether they were tested under high strain-rate loading or fold recovery. Across the full landscape of these observables, molecular architecture played a more influential role than the hard-soft segment composition ratio. Understanding these material characteristics is vital to the design of next generation microphase-separated materials for use in both ballistic shields and face masks for soldier protection.

1. INTRODUCTION

Polyurethane chemistries are versatile and multi-functional, particularly for segmented polyurethanes, which generally consist of copolymers of solid-like hard and rubbery soft segments of various sequence lengths. Microphase separation as a result of thermodynamic incompatibility between these segments gives rise to a broad range of useful physical and mechanical properties. The type and molecular weight of diisocyanates and chain extenders used in the synthesis of hard segments, and the choice of polyether- or polyester-based polyols for soft segments, affect the morphology and bulk properties of segmented polyurethanes (James Korley et al., 2006; Martin et al., 1996; Miller and Cooper et al., 1985; Wang and Cooper et al., 1983; Schneider et al., 1975; Abouzahr and Wilkes et al., 1982; Byrne, et al. 1991; Duffy et al., 1990; Meckel et al., 1996; Martin et al., 1996). Aromatic diisocyanates tend to render the soft segments of segmented polyurethanes difficult to crystallize upon cooling, while the aliphatic counterparts generally provide less hindrance towards crystallization (Lee et al., 2000). Polyurethanes made from aromatic diisocyanates are also more mechanically robust; however, aliphatic-based polyurethanes offer excellent outdoor UV and light stability over long-term service exposure (Meckel et al., 1996). These materials have found extensive usage in both military and commercial applications in the areas of

Report Documentation Page

Form Approved
OMB No. 0704-0188

1. REPORT DATE	2. REPORT TYPE	3. DATES COVERED
01 NOV 2006	**N/A**	**-**

4. TITLE AND SUBTITLE	5a. CONTRACT NUMBER
Unraveling Dynamic Mechanical Deformation In Segmented Polyurethanes: From High Strain-Rate Hardening To Complete Fold Recovery	5b. GRANT NUMBER
	5c. PROGRAM ELEMENT NUMBER
6. AUTHOR(S)	5d. PROJECT NUMBER
	5e. TASK NUMBER
	5f. WORK UNIT NUMBER
7. PERFORMING ORGANIZATION NAME(S) AND ADDRESS(ES) **U. S. Army Research Laboratory, AMSRD-ARL-WM-MD Aberdeen Proving Ground, MD 21005-5069**	8. PERFORMING ORGANIZATION REPORT NUMBER
9. SPONSORING/MONITORING AGENCY NAME(S) AND ADDRESS(ES)	10. SPONSOR/MONITOR'S ACRONYM(S)
	11. SPONSOR/MONITOR'S REPORT NUMBER(S)

12. DISTRIBUTION/AVAILABILITY STATEMENT
Approved for public release, distribution unlimited

13. SUPPLEMENTARY NOTES
See also ADM002075., The original document contains color images.

14. ABSTRACT

15. SUBJECT TERMS

16. SECURITY CLASSIFICATION OF:			17. LIMITATION OF ABSTRACT	18. NUMBER OF PAGES	19a. NAME OF RESPONSIBLE PERSON
a. REPORT	b. ABSTRACT	c. THIS PAGE			
unclassified	**unclassified**	**unclassified**	**UU**	**7**	

barrier materials, fibers, hard coatings and engineering thermoplastics (Simula, 2006; DuPont, 2006).

The current U.S. Army Joint Service General Purpose Mask (JSGPM) program requires a lens system that can be folded while providing a high level of optical quality, chemical resistance, ballistic eye protection, flame resistance, scratch resistance, and environmental durability. Reaction-cast polyurethanes have been selected under JSGPM to replace polycarbonate as lens materials for field evaluations (Figure 1). Results showed that some of these polyurethane materials had outstanding impact strength but they could not unfold rapidly and completely from bend deformation or storage over an extended period of time (Grove, 1999). On the other hand, those with complete fold-recovery capability were found to possess insufficient chemical and ballistic protective properties (Grove, 1999). Fold recovery capability is an important characteristic of the JSGPM since the ability to fold in as small a package as possible and unfold rapidly and completely when needed is imperative particularly for first response teams and special force operations.

Fig. 1 Joint Service General Purpose Mask

Polyurethanes have also been developed for use in the transparent lightweight ballistic shields applications (Dehmer et al., 2000; Simula, 2006). Despite the ballistic performance of these polyurethane materials in the form of monolithic sheets, recent ARL research studies have revealed that laminates made from these PU materials did not perform as well as the hard/ductile composites that had equivalent overall areal density and were prepared from using PMMA as a front plate and PU as a back-support layer. The high strain-rate sensitivity of PMMA was attributed to the improved overall ballistic performance of PMMA/PU composites over the corresponding PU/PU configuration (Hsieh et al, 2004).

In this work, we have systematically evaluated a selected set of model polyurethanes to determine the influence of molecular structure, in contrast to increasing hard segment content, on glass transition temperature, viscoelastic relaxation and mechanical deformation. Microphase separated morphology was examined by both wide-angle X-ray scattering (WAXS) and small-angle X-ray (SAXS) scattering. Thermal transition temperatures were determined by differential scanning calorimetry (DSC). The frequency dependence of molecular relaxation was determined by both dynamic mechanical analysis (DMA) and dielectric analysis (DEA) techniques. Results from these measurements were used to correlate and interpret the rate-dependent properties of these PU's when tested under very different mechanical loading conditions, namely uniaxial compression and fold recovery from bend deformation. The objective of this work is to determine the molecular mechanisms that are critical for mechanical strengthening, thus to enable the design of segmented polyurethanes with improved materials survivability for protection against emerging threats.

2. EXPERIMENTAL

2.1 Materials

Polyurethane materials with controlled variation in hard segment content and different chain extenders were the subjects of this study. The details of material synthesis and sample preparation can be found elsewhere (Yi et al., 2006). In general, these polyurethanes consist of poly-carbodiimide-modified diphenylmethane diisocyanate, (ISONATE^{TM} 143L modified MDI, Dow Chemical) and poly(tetramethylene ether) glycol, PTMG, (Terathane® 1000, DuPont). The ISONATE^{TM} 143L modified MDI is liquid at room temperature, and it contains polycarbodiimide adduct linkages capable of providing PU with stabilization against hydrolytic degradation (Dow Chemical, 2006). The chain extenders used included 1,4-butanediol (BDO, Sigma-Aldrich) and 2,2-dimethyl-1,3-propanediol (DMPD, Sigma-Aldrich). Three polyurethanes, PU-B-54, PU-D-55, and PU-B-44 were selected for evaluation. The sample nomenclature includes B and D for the chain extenders BDO and DMPD, respectively, and the numerals reflect the hard segment content that varies from 44 to 55 wt.% in these PU's. Compression molded sheets of about 6 mm thick were used for material characterization and mechanical testing.

2.2 Characterization

The ISONATE 143L modified MDI contains polycarbodiimide adduct linkages which can undergo reversible formation and dissociation reactions at about 90 °C (Dow Chemical, 2006). Therefore, all the DSC, DMA and DEA measurements were conducted at temperatures below 80 °C to avoid undesirable chemical changes. Differential scanning calorimetry measurements were performed in modulated-DSC mode using a TA Instruments Q1000 DSC, in order to eliminate the influence of thermal history and physical aging, and to ensure that accurate thermal transition temperatures were

obtained directly from the first heating scans. PU samples of 10-15 mg were heated at 3 °C/min with a modulation of ±0.3 °C every 60 seconds over the temperature range of -90 to 80 °C. Dynamic mechanical analysis was carried out using a TA Instruments Q800 DMA in tension mode. Rectangular specimen geometry with dimensions of 3 mm width, 2 mm thickness and with a gauge length of 9 mm was employed. Measurements of dynamic mechanical properties were conducted at constant strain amplitude of 0.1% and scanned at a fixed frequency of 1, 10 and 100 Hz from -156 to 80 °C at a heating rate of 3 °C/min. Dielectric analysis operated at multi-frequency mode was carried out using a TA Instruments DEA 2970. Parallel plate sensors were employed and a maximum force of 250 N was applied to each 1 mm thick sample. The sample was preheated to 55 °C to ensure better surface contact with sensors and then cooled to -100 °C, followed by scanning at a rate of 2 °C/min at selected frequencies of 1, 3, 10, 30, 100, 300, 1000, 3000, and 10000 Hz. Capacitance and conductance were measured to obtain the permittivity (ε′), the dielectric loss (ε″) and the tanδ (=ε″/ε′). For simplicity, the term glass transition temperature, T_g, is used when comparing the glass or α transition temperature data obtained from DSC, DEA and DMA. Uniaxial compression measurements at constant strain rate were conducted on an Instron 1350 servo-hydraulic test machine using a true strain rate control mode. The compression specimens were 12 mm in diameter and 6 mm in height. Small-angle X-ray scattering measurements were performed using a Molecular Metrology SAXS equipped with CuKα radiation and a two-dimensional, gas proportional multi-wire Gabriel detector. Variations in beam intensity were corrected by subtracting the normalized background radiation. The transmission factor was obtained from intensity measurements using a photodiode placed on the beam stop. The sample-to-detector distance was 1094 mm. Wide-angle X-ray scattering data were collected using the above configuration with the insertion of a Fuji image plate between the sample and SAXS detector, at a distance of 105 mm. A hole bored in the center of the WAXS image plate allowed for passage of the small-angle reflections to the SAXS detector.

The ability of these model PU samples to recover from bending deformation was measured following the test procedure recommended by ASTM D6515-00 (ASTM, 2004). The ends of rectangular specimens of dimensions 50 mm x 25 mm x 1 mm were secured with binder clips and then maintained under folded conditions for selected periods of time. Evaluation of fold recovery was performed by taking photographs to record the unfolding events as a function of time.

3. Results and Discussion

3.1 Morphology Analysis and Thermal Characterization

The polycarbodiimide-modified MDI has an aromatic nature similar to MDI, and additionally has average isocyanate functionality greater than two (Dow Chemical, 2006). Therefore, it was anticipated that the hard segments in these model PU samples would be less well-packed compared with other aliphatic diisocyanate-based PUs. Indeed, this is consistent with the wide-angle X-ray data, in which a similar broad reflection with a Bragg spacing of 4.3 Å is observed for all three PU samples. On the other hand, the small-angle X-ray scattering data, shown in Figure 2, reveal that the interdomain structure varies substantially across the series. Samples PU-B-54 and PU-B-44, which both possess the chain extender 1,4-butanediol (BDO), exhibit a broad scattering peak typical of phase-separated segmented polyurethanes. This peak has been assigned to the spacing between hard-segment domains within the soft-segment continuous matrix. The interdomain spacing is 11 nm for PU-B-54, and shifts to a larger distance, 13 nm, for PU-B-44 as a result of lower hard segment content. Sample PU-D-55, in contrast, with the chain extender DMPD, exhibits no scattering peak in the small-angle region. This suggests a lack of significant interdomain correlations due to greater phase mixing. The influence of chain extender chemistries is also evidenced in the DSC data. The BDO-containing samples, PU-B-54 and PU-B-44, show similar soft segment glass transition temperatures (T_g), at -36 °C and -34 °C, respectively. On the other hand, sample PU-D-55 displays a soft segment T_g at much higher temperature of 15 °C. This increase of 51 °C in soft segment T_g of sample PU-D-55 over PU-B-54 again suggests that the steric effect associated with the pendant methyl groups in DMPD results in an altered packing of the hard segment regions, thus leading to better phase mixing between the hard and soft segments. Both SAXS and DSC results clearly indicate that the influence of DMPD in the shift of soft segment T_g as well as in the packing order of hard segments is more significant in comparison to the increasing of hard segment content.

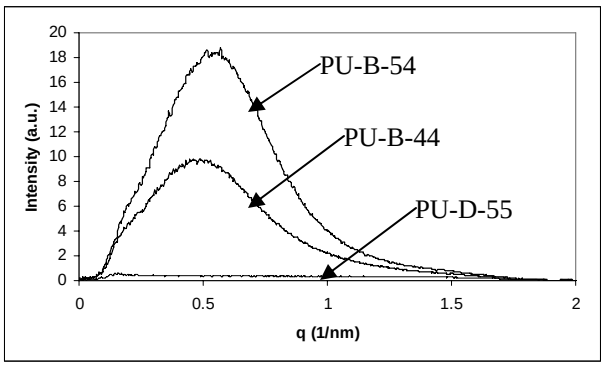

Fig. 2. SAXS data of PU-B-54, PU-D-55, and PU-B-44.

3.2 Molecular Relaxation

Measurements of viscoelastic relaxation were carried out by both DMA and DEA. While DMA usually performs at frequencies below 100Hz, DEA on the other hand can operate up to 10^6 Hz. Therefore, for polymers containing dipolar groups, DEA which measures the change of polarization in an electric field can complement the DMA in probing the same segmental relaxation but at higher frequencies (McCrum et al., 1991). Figure 3 depicts a plot of the tanδ vs. temperature data obtained by DMA at frequencies of 1 Hz and 10 Hz. Increasing the hard segment content slightly increases the soft segment glass transition temperature of PU-B-54 over PU-B-44 at all frequencies. However, incorporation of DMPD chain extender yields PU-D-55 with a glass transition temperature much higher than PU-B-54 and PU-B-44, as seen in DSC. The glass transition temperature increases with increasing frequency; moreover, the tanδ values increase with either hard segment content or chain extender DMPD incorporation. Both are correlated to a decrease in phase separation or improved phase mixing as indicated by the SAXS data. Therefore, the greater the phase mixing in these model PU's, the higher the dynamic mechanical relaxation strength at all frequencies. The frequency dependence of molecular relaxation is also evidenced in the dielectric (DEA) measurements. The glass transition temperature data are consistent in both DEA and DMA. Figure 4 is a typical plot of tanδ vs. temperature data obtained from DEA. It is noteworthy that T_g of PU-B-54 remains below 10 °C even as frequency increases to 10,000 Hz, similar to PU-B-44, yet T_g of PU-D-55 reaches room temperature when frequency is as low as 1-3 Hz. These results suggest that PU-D-55, relative to the BDO-containing samples, changes more rapidly from leathery to glassy as frequency increases. Therefore, varying the extent of phase mixing by changing the molecular compatibility between hard and soft segments plays a larger role in the rate dependence of molecular relaxation when compared with the influence of altering the hard segment content.

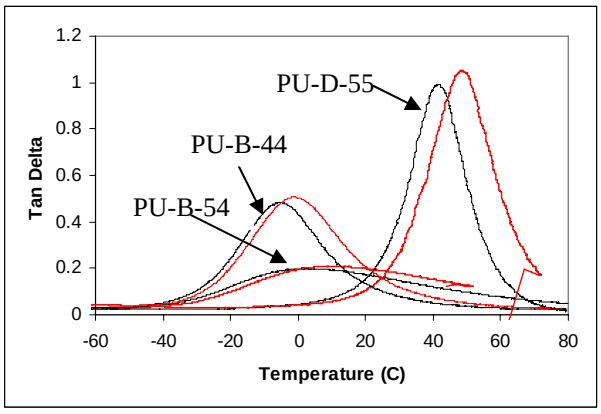

Fig. 3. DMA data obtained at 1 Hz (black) and 10 Hz (red) for samples PU-B-54, PU-D-55, and PU-B-44.

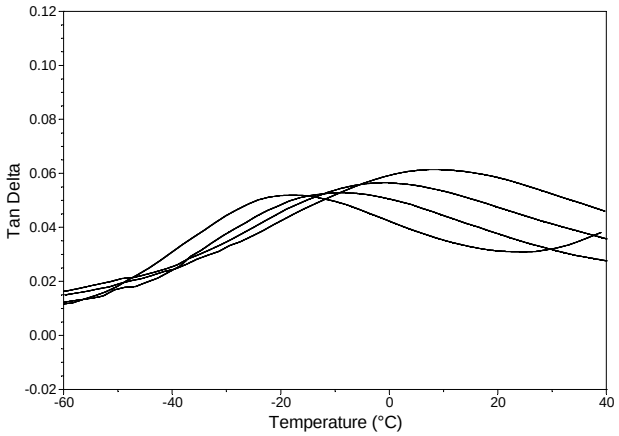

Fig. 4. DEA data for sample PU-B-54, obtained at dielectric frequency of 10, 100, 1,000 and 10,000 Hz; frequency increased for curves from left to right.

3.3 Mechanical Deformation

The mechanical response of segmented polyurethanes can be altered greatly based on the choice of hard and soft segments and their compositions. In this work, we focus on two aspects of mechanical deformation including rate-sensitivity under uniaxial compression and fold recovery after bend deformation.

3.3.1 Compression Measurements

The influence of molecular structures on quasi-static and high strain-rate compression was examined in these model segmented PUs. Both BDO-containing PU-B-54 and PU-B-44 samples exhibited little change in initial stiffness over the strain rate 10^{-2}–1 s^{-1} (Figure 5). On the other hand, PU-D-55 with DMPD has the lowest value of yield stress among the three at room temperature, yet it displayed a drastic change in stiffness over the same quasi-static regime (Figure 5). Sample PU-D-55 displayed rubbery-like deformation at 10^{-2} s^{-1} but it became leathery-like at 1 s^{-1}. These results indicate that the strain-rate sensitivity of increasing stiffness or flow stress is significantly dependent upon the extent of physical mixing between hard and soft segments; furthermore, the molecular influence is much more dominant than the variation of hard segment content. The molecular dependence of strain-rate hardening is also consistent in the high strain-rate deformation measured by split Hopkinson-bar compression (Yi et al., 2006). At strain rate 10^3 s^{-1}, PU-B-44 appeared leathery-like and PU-B-54 with higher hard segment content became nearly glassy, while the DMPD-containing PU-D-55 turned out to be completely glassy. Figure 6 compares the flow stress taken at strain 0.15 and the DMPD-containing PU exhibits the highest strain-rate sensitivity among these model PU samples (Yi et al., 2006).

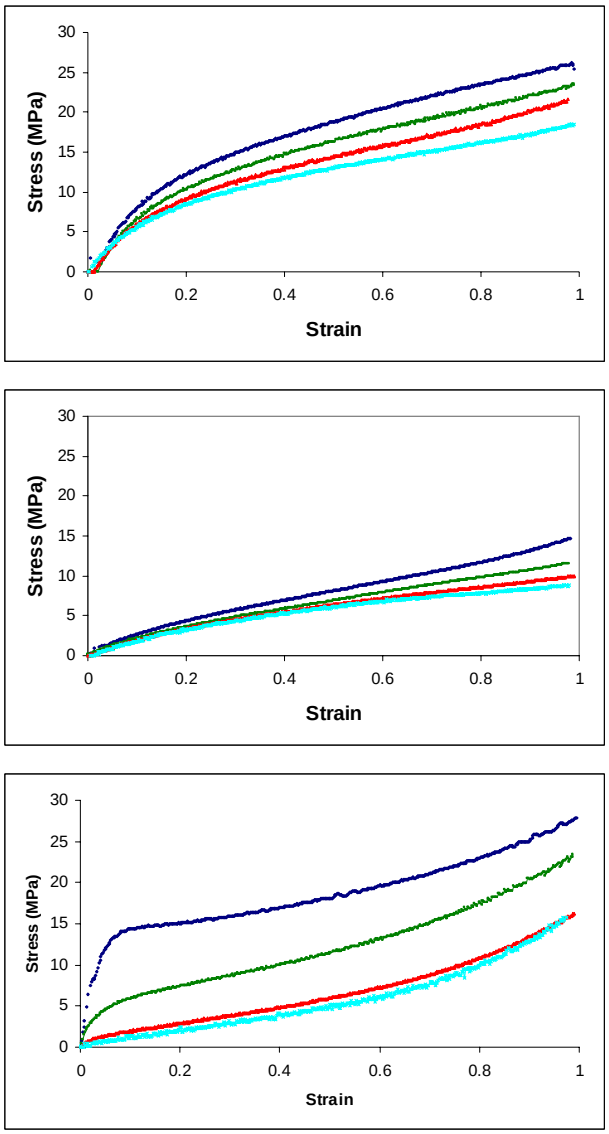

Fig. 5. Compression stress-strain data for PU-B-54 (top), PU-B-44 (middle), and PU-D-55 (bottom) obtained at strain rates 0.002 (turquoise), 0.01 (red), 0.1 (green) and 1 (blue) s^{-1} (Yi et al., 2006).

3.3 Fold Recovery

As mentioned above, face masks with complete fold recovery capability in addition to chemical/biological barrier properties are critical for the first response team during mission-critical conditions. Measurements of the ability to recover from bend deformation were conducted for samples after being folded with binder clip for selected periods of time. A profound difference in fold recovery, induced by merely altering the chain extender, was apparent. Figure 7 are photographs taken before and after samples first folded with a binder clip for two minutes and then recovered after 30 seconds from stress release. Both PU-B-54 and PU-B-44 samples unfolded rapidly and completely, while PU-D-55 underwent unfolding at a much slower rate.

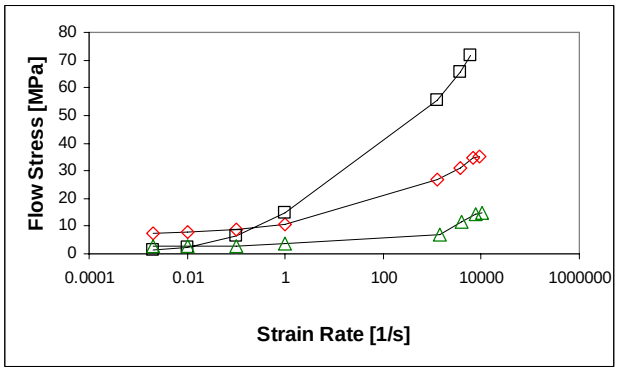

Fig. 6. Flow stress (taken at strain 0.15) vs strain rate data for BDO-containing PU's with 54 wt.% (◊) and 44 wt.% (Δ) hard segment content, and for DMPD-containing PU with 55 wt.% (□) hard segment content (Yi et al., 2006); flow stress values at 0.002 s^{-1} are 7.3 MPa, 2.6 MPa and 1.6 MPa for PU-B-54 (◊), PU-B-44 (Δ) and PU-D-55 (□), respectively, which were used for correlation with apparent crosslink density and fold recovery data.

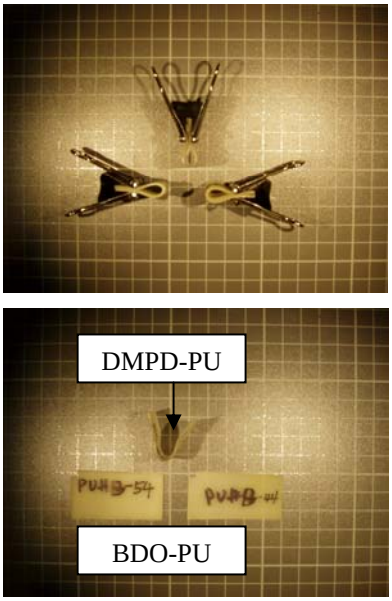

Fig. 7. Photographs taken from fold recovery measurements showing clamped (top) and unfolded (bottom) PU samples.

The fold-recovery behavior correlated well with the apparent crosslink density (ν_e) estimated from the rubbery plateau modulus data from DMA based on the following equation derived from rubber elasticity theory for the ideal crosslinked networks (Sperling, 1986; Chen, 2006)

$$\nu_e = E' / 3RT \quad (T >> T_g) \qquad (1)$$

where R is the gas constant, T is the temperature and E′ is the modulus for crosslinked polymers taken at

temperatures well above T_g. The ν_e values calculated based on rubbery plateau modulus (E_b) data at 75 °C are listed in Table 1. Incorporation of DMPD resulted in significantly lower apparent crosslink density than the BDO-containing PU samples: PU-D-55 has only one-sixth the effective crosslink density of PU-B-54, despite their similar hard segment contents. The material response under fold-recovery resembled the low strain-rate deformation observed at 0.002 s^{-1} (Figure 6), and both were dominated by the apparent crosslink density of these model PUs. Samples PU-B-54 and PU-B-44 have higher flow stress (7.3 MPa and 2.6 MPa, respectively) than PU-D-55 (1.6 MPa), and both BDO-containing PUs recovered easily from fold deformation. On the contrary, increasing the apparent crosslink density via an increase in microphase separation caused a significant decrease in strain-rate sensitivity. These experimental findings clearly demonstrate that the extent of phase mixing is critical to segmented polyurethanes over the full spectra of mechanical deformation from high strain-rate hardening to complete fold recovery.

Table 1. DMA rubbery plateau modulus (E_b) data and values of apparent crosslink density of PU samples calculated from Eqn.1.

	E_b (MPa) at 75 °C from DMA	ν_e (mol/M^3)
PU-B-54	52.4	6.0
PU-D-55	7.9	0.9
PU-B-44	18.5	2.1

CONCLUSIONS

Mechanical deformation measurements, as well as morphology characterization, thermal analysis and molecular relaxation were carried out on selected model segmented polyurethanes. The extent of phase mixing appeared to be the predominant molecular mechanism that affected the mechanical deformation in terms of both the high strain-rate hardening and fold recovery considerably among these model segmented polyurethanes. Better phase mixing between the hard and soft segments occurred when DMPD was used as a chain extender. This was verified by both DSC and SAXS data. PU samples containing DMPD had no significant interdomain correlations but the BDO-containing PU samples displayed the broad scattering peak typical of segmented polyurethanes. Furthermore, the greater the phase mixing in these model PUs, the higher the dynamic mechanical relaxation strength at all frequencies.

PU sample with DMPD had the lowest value of yield stress at room temperature; however, it displayed a drastic increase in stiffness as strain rate increases. This DMPD-containing PU sample appeared to be rubbery-like mechanical deformation at 10^{-2} s^{-1}, then leathery-like at 1 s^{-1} and became completely glassy as strain rate reached 10^3 s^{-1}. Furthermore, varying the extent of phase mixing by changing the molecular compatibility between hard and soft segments played a larger role in the rate dependence of molecular relaxation when compared with the influence of altering of the hard segment content. These observations suggest that polyurethanes with greater phase mixing will be more effective engineering materials when high strain-rate-dependent properties are required, and hence incorporating PUs with improved dynamic hardness will be favorable in the design of hard/ductile hybrids for ballistic shield applications.

Increasing the hard segment content alone led to higher flow stress, improved fold recovery but lower dynamic mechanical relaxation strength. On the contrary, increasing the phase mixing by merely altering the chain extender to DMPD resulted in substantially higher relaxation strength and strain-rate sensitivity yet was found detrimental to fold recovery among these model segmented polyurethanes. These findings clearly demonstrate that the current segmented PU technology is not capable of providing flexible lenses with both desired properties of high strain-rate mechanical hardening and complete fold recovery. Hence, exploiting new molecular mechanisms as an alternate approach is essential and will be undertaken in the design of hierarchical hybrid structures that can fulfill the full spectra of physical and mechanical deformation requirements.

ACKNOWLEDGEMENTS

We thank Drs. G.F. Lee and E. Balizer, Naval Surface Warfare Center, Silver Spring, MD for providing the polyurethane samples used in this work, and U.S. Army Natick Soldier Center, Natick, MA for utilizing their TA Instruments DEA 2970 to perform dielectric analysis measurements. Pate and Yi acknowledge the support by the Army through the Institute for Soldier Nanotechnologies under contract DAAD-19-02-D0002, and by the Office of Naval Research through grant N00014-04-10469, respectively. The content of this research does not necessary reflect the position of the Government, and no official endorsement should be inferred.

REFERENCES

Abouzahr S., Wilkes G. L., Ophir, Z., 1982: Structure-Property Behavior of Segmented Polyether-MDI-Butanediol Based Urethanes: Effects of Composition Ratios, Polymer, 23, 1077-85.

ASTM D6515-00, 2004; Standard Test Method for Rubber Shaft Seals Determination of Recovery from Bending.

Byrne C. A., Desper C. R., Mead J. L., 1991; Structure Property Relationship of Aliphatic Polyurethane Elastomers Prepared from CHDI, U.S. Army Research Laboratory, Technical Report, MTL-TR-91-26.

Chen Y., Zhou S., Gu G., Wu L., 2006; Microstructure and Properties of Polyester-based Polyurethane/titania Hybrid Films Prepared by Sol-Gel Process, Polymer, 47-1640-48.

Dehmer P. G., Klusewitz M., 2000: High Performance Visors, Proceedings, 8th DOD Electromagnetic Windows Symposium, USAF Academy.

Dow Chemical Company, 2006; ISONATE 143L Product Information.

Duffy J. V., Lee G. F., Lee J. D., Hartmann B., 1990: Dynamic Mechanical Properties of Poly(tetramethylene ether) Glycol Polyurethanes, American Chemical Society Symposium Series, 424, Edited by Corsaro R. D., Sperling L. H., 281-293.

DuPont Terathane Products, 2006; Technical Information.

Grove C. M., 1999: Material Study for the Joint Service General Purpose Mask, U.S. Army Edgewood Chemical Biological Center, Technical Report, ECBC-TR-043.

Hsieh A. J., DeSchepper D., Moy P., Dehmer P. G., Song J. W., 2004: The Effect of PMMA on Ballistic Impact Performance of Hybrid Hard/Ductile All-Plastic and Glass-Plastic-Based Composites, U.S. Army Research Laboratory, Technical Report, ARL-TR-3155.

James Korley L. T., Pate B. D., Thomas E. L., Hammond P. T., 2006; Effect of the Degree of Soft and Hard Segment Ordering on the Morphology and Mechanical Behavior of Semicrystalline Segmented Polyurethanes, Polymer 47, 3073-82.

Lee D.K., Tsai H. B., 2000: Properties of Segmented Polyurethanes Derived from Different Diisocyanates, J. Apply. Polym. Sci., 75, 167-74.

Martin D. J., Meijs G. F., Renwick G. M., McCarthy S. J., Gunatillake P. A., 1996: The Effect of Average Soft Segment length on Morphology and Properties of a Series of Polyurethane Elastomers. I. Characterization of the Series, J. Appl. Polym. Sci., 62, 1377-86.

Meckel W., Goyert W., Wieder W., 1996: Thermoplastic Polyurethane Elastomers, in "Thermoplastic Elastomers", 2nd ed., Edited by Holden G., Legge N. R., Quirk R., Schroeder H. E., Hanser/Gardner, Cincinnati, OH.

Miller J. A., Lin S. B., Hwang K. K. S., Wu, Gibson P. E., Cooper S. L., 1985: Properties of Polyether-Polyurethnae Block Copolymers: Effects of Hard Segment Length Distribution, Macromolecules, 18, 32-44.

McCrum N. G., Read B. E., Williams G., 1991: Anelastic and Dielectric Effects in Polymeric Solids, Dover Publications, Inc., New York.

Schneider N. S., Desper C. R., Illinger J. L., King A. O., Barr D., 1975: Structural Studies of Crystalline MDI-Based Polyurethanes, J. Macromol. Sci.-Phys., B11, 527-52.

Simula, Inc., 2006: Cleargard™ Products data sheet.

Sperling L. H., 1986: Introduction to Physical Polymer Science, John Wiley & Sons, Inc., New York.

Wang C. B., Cooper S. L., 1983: Morphology and Properties of Segmented Polyether Polyurethanes, Macromolecules, 16, 775-86.

Yi J., Boyce M. C., Lee G. F., Balizer E., 2006; Large Deformation Rate-Dependent Stress-Strain Behavior of Polyurea and Polyurethanes, Polymer, 47, 319-29.